AIAA JOURNAL
Vol. 46, No. 7, July 2008

# Modeled Boltzmann Equation and Its Application to Direct Aeroacoustics Simulation

S. C. Fu,* R. M. C. So,† and R. C. K. Leung‡
*Hong Kong Polytechnic University,*
*Hung Hom, Hong Kong, People's Republic of China*

DOI: 10.2514/1.33250

**The Bhatnagar, Gross, and Krook modeled Boltzmann equation has been applied to simulate different fluid dynamics problems with varying degrees of success. However, its application to direct aeroacoustic computation is less successful. One possible reason could be its inability to recover the state equation correctly for a diatomic gas and hence an inaccurate determination of the speed of sound. The present study reports on the development of an improved modeled Boltzmann equation for aeroacoustics simulation. The approach is to modify the Maxwellian distribution normally assumed for the equilibrium particle distribution function. Constraints imposed are the exact recovery of the state equation for a diatomic gas and the Euler equations without invoking the small Mach number assumption. Thus formulated, a distribution function consisting of the Maxwellian distribution plus three other terms that attempt to account for particle–particle collisions is obtained. A velocity lattice method is used to solve the improved modeled Boltzmann equation using an equivalent lattice equilibrium distribution function. The simulations are validated against benchmark aeroacoustic problems whose solutions are deduced from a direct numerical simulation of the Euler equations. The results of the improved modeled Boltzmann equation obtained using a smaller computational domain are in excellent agreement with those deduced from direct numerical simulation using a larger computational domain, thus verifying the viability and correctness of the modified equilibrium distribution function.**

## Nomenclature

| | | |
|---|---|---|
| $C_p$ | = | specific heat at constant pressure |
| $c$ | = | speed of sound |
| $D$ | = | problem dimension |
| $D_T$ | = | translational degree of freedom of the particle |
| $D_R$ | = | rotational degree of freedom of the particle |
| $e$ | = | internal energy |
| $f$ | = | particle distribution function |
| $f^{\text{eq}}$ | = | equilibrium particle distribution function |
| $Kn$ | = | Knudsen number |
| $L$ | = | characteristic length |
| $M$ | = | Mach number |
| $p$ | = | pressure |
| $R$ | = | universal gas constant |
| $T$ | = | gas temperature |
| $t$ | = | time |
| $\mathbf{u}$ | = | fluid velocity vector |
| $u$ | = | stream velocity component |
| $v$ | = | normal velocity component |
| $\mathbf{x}$ | = | position vector |
| $x$ | = | stream coordinate |
| $y$ | = | normal coordinate |
| $\gamma$ | = | specific heat ratio |
| $\theta$ | = | normalized temperature, $RT$ |
| $\kappa$ | = | fluid conductivity |
| $\mu$ | = | fluid shear viscosity |
| $\boldsymbol{\xi}$ | = | particle velocity vector |
| $\rho$ | = | fluid density |
| $\sigma$ | = | lattice velocity magnitude |
| $\tau$ | = | relaxation time |

*Subscripts*

| | | |
|---|---|---|
| $i, j$ | = | vector and/or tensor indices |
| $o$ | = | microscopic reference condition |
| $r$ | = | macroscopic reference condition |
| $\alpha$ | = | index for the lattice velocity |
| $\infty$ | = | upstream reference condition |

Received 3 July 2007; revision received 5 January 2008; accepted for publication 5 January 2008. 

*Research Assistant, Department of Mechanical Engineering.

†Professor Emeritus, Department of Mechanical Engineering, and Industrial Center, Corresponding Author; mmmcso@polyu.edu.hk. Fellow AIAA.

‡Assistant Professor, Department of Mechanical Engineering. Senior Member AIAA.

## I. Introduction

DIRECT aeroacoustic simulation (DAS) is much more difficult and demanding because of scale disparity and the necessity to resolve the acoustic disturbances correctly [1]. Therefore, numerical errors have to be at least equal to or less than $10^{-5}$ to allow an accurate resolution of the acoustic disturbances to be obtained. Numerical schemes which are accurate enough for this purpose have been proposed by Lele [2], Tam and Webb [3], and Visbal and Gaitonde [4]. Since then, computational aeroacoustics have been carried out by numerically solving either the Euler or Navier–Stokes (NS) equations directly [1,5].

Recently, the modeled Boltzmann equation (MBE) has developed into a promising alternative to the Euler and NS equations for simulating aerodynamic flows, and laminar and turbulent fluid dynamic flows [6–8]. This is because of the simplicity of the Bhatnagar, Gross, and Krook (BGK) model [9] and the ability of the MBE to recover the macroscopic governing fluid flow equations assuming a lattice $f^{\text{eq}}$ and using a velocity lattice numerical method to solve the single scalar equation for $f$. This lattice Boltzmann method (LBM) has drawbacks: chief among them are the monatomic gas and very small $M$ stipulations embodied in the assumed lattice $f^{\text{eq}}$. Thus, its application to simulate aeroacoustic problems is in doubt. Even then, attempts have been made to use the LBM to tackle aeroacoustic problems [10–13]. However, the results are not very satisfactory because the LBM could not correctly recover $\gamma$ or $\mu$ over

the whole field, and $M \ll 1$ is inherent in the lattice $f^{eq}$, thus limiting the applications to a narrow range of small $M$. Attempts to remedy some of these shortcomings have been made by considering a rotational degree of freedom in the model and by invoking the Sutherland law as a constraint [14–16]. In spite of these improvements, $M \ll 1$ is still inherent in the assumed lattice $f^{eq}$. Therefore, it is clear that, if the MBE were to be a viable alternative to the Euler or NS equations for DAS, there is a need for an alternative formulation in which the monatomic gas and $M \ll 1$ assumption is not required in the solution of the MBE.

To further explore the viability of the proposed $f^{eq}$ and the inherent monatomic gas and $M \ll 1$ assumptions, a brief review of the work that has been carried out in the analytical approach to extend the MBE to polyatomic gas and the use of the lattice method to remedy the drawbacks for aeroacoustic simulations is necessary. The analytical approach is reviewed first and this is followed by a discussion of the LBM. From this review, an approach to derive an alternative $f^{eq}$ and its lattice counterpart is identified for the present study.

In principle, the original Boltzmann equation (BE) is valid for polyatomic gas [17]. The solution of $f$ should also be valid for polyatomic gas if the collision integral on the right-hand side of the BE could be modeled to include the nonlinear physics of the particle collision processes. As such, the BE should be equally applicable for aeroacoustic problems, as long as the Euler and NS equations can be recovered from the BE with no restrictions imposed to compromise the MBE. After all, the wave equation is a subset of the Euler or NS equations. The minimum requirement then is the ability of the MBE to recover the acoustic scaling form of the Euler and/or NS equations [18]. The drawbacks of the current MBE is a consequence of the oversimplification of the BGK modeling of the collision integral; it models the collision integral by stipulating that $f$ only deviates slightly from $f^{eq}$ and that sufficient collision physics have been modeled in the proposed $f^{eq}$ to allow a correct recovery of the Euler and NS equations. This concept is valid, provided the proposal for $f^{eq}$ is general enough. However, the original BGK model only considers the energy mode due to inelastic translational collisions; therefore, it renders the resulting MBE valid for monatomic gas and the need to invoke $M \ll 1$ in the recovery of the Euler and NS equations.

Although the kinetic theory of polyatomic gas, especially diatomic gas, is important for aerodynamic and acoustic problems, relatively little work, other than those on monatomic gas, has been carried out on their applications to aeroacoustics. This is because work on polyatomic gas would involve a generalization of the MBE to include as many energy modes as mathematically possible. When the rotational angular momentum is taken into account in the derivation of $f^{eq}$, the resulting theory could be too complicated, especially for numerical purposes. Wang Chang, Uhlenbeck, and deBoer (WCUB) [19] suggested a WCUB equation by introducing a set of $f$ for each quantum mode to specify the internal state of the particles. This equation is based on a spherically symmetric interparticle potential, and it yields an appropriate description for polyatomic gas. However, their formulation does not take into account the polyatomic gas with significant dipole moments or with degenerating internal state [20]. This is in spite of the fact that the degenerate rotational states do play an essential role in the angular momentum polarizations. The WCUB equation has been used by other researchers as a base to formulate other models and approaches.

To improve the applicability of the WCUB approach, Morse [21] simplified the WCUB equation using a BGK-type MBE. Later, Holway [22] constructed an ellipsoidal statistical BGK model, and applied it to the equation developed by Morse [21] to obtain a correct $\kappa$. This was achieved by replacing the Maxwellian distribution function with an anisotropic Gaussian distribution. All of these approaches, including the WCUB, encountered difficulties in numerical applications because their proposed $f^{eq}$ is a set of Maxwellian distribution functions corresponding to different internal states. If the velocity lattice method were used to solve this MBE, there is no clear indication on how a corresponding lattice $f^{eq}$ could be derived. As a result, these approaches are seldom used to solve practical fluid dynamic problems. Nevertheless, the idea of considering multi-energy modes, instead of angular momentum alone, to account for various internal degrees of freedom is extensively employed in gas-kinetics schemes.

Xu and Prendergast [23–25] developed a family of finite volume gas-kinetic schemes based on the BGK model for the compressible NS equations. Instead of using a set of distribution functions, they introduce an internal variable to account for the internal degree of freedom in polyatomic gas. The internal variable is particularly useful in the derivation of the NS equations, and would not appear in the final formulation of the scheme. The $f^{eq}$ is assumed to be a modified Maxwellian. A second-order-accurate scheme was developed. Theoretically, interpolation techniques used to construct the subcell structure can extend the scheme to higher-order resolution and hence suitable for DAS.

The LBM approach to solve the MBE is considered a particular discretization for the discrete BE with second-order accuracy in both space and time [26]. The discrete BE by nature is, in fact, a system of inhomogeneous hyperbolic equations with nonlinear source terms. In principle, higher-order-accurate solution of the discrete BE can be achieved through the use of higher-order schemes. Various higher-order numerical schemes have been proposed, and this includes a higher-order compact-differencing and filtering algorithm, coupled with a fourth-order Runge–Kutta scheme for simulating aeroacoustic problems [2–4,27]. Therefore, numerically solving the MBE to resolve the acoustic disturbances is no longer an obstacle [14–16]. However, accurate resolution of aeroacoustic properties still lies in the ability of the BGK-type MBE to mimic correctly the physics of aeroacoustics and its interaction with aerodynamic disturbances and structural dynamics.

In the LBM approach to solve the MBE, some researchers choose to employ the concept of the energy mode to facilitate a free choice of $\gamma$ and hence a tacit extension of the BGK model to polyatomic gas. Tsutahara et al. [13] proposed the use of one additional distribution function to simulate the internal degree of freedom, and a finite difference lattice Boltzmann scheme was employed to solve the resulting equation. On the other hand, shock capturing schemes based on LBM with a multi-energy level were proposed to treat the fully compressible Euler equations [28–30]. A similar technique, incorporating flexible $\gamma$ and assuming a multi-energy level to correspond to multilattice speed, is employed by Kataoka and Tsutahara [11] to recover the NS equations, and they used an LBM to solve the MBE for aeroacoustic problems. The lattice approach has also been used to remedy the small $M$ assumption and to treat high-speed flow problems [30]. Recovery of macroscopic physical laws from the MBE with flexible $\gamma$ was determined by introducing variable quantities related to energy levels rather than by assuming a set of distribution functions. These variable quantities are mainly introduced to facilitate numerical solutions and for ease of mathematical manipulation; however, their physical meanings are not clear. These approaches only concentrate on the discrete BE; the recovery of the Euler and the NS equations from the continuous form of the BE and the associated $f^{eq}$ are not available. Therefore, these approaches are not as appropriate for aeroacoustic simulations as the finite volume gas-kinetic schemes [23–25].

This brief review indicates that the BGK-type MBE, with appropriate modifications made to the continuous $f^{eq}$, could become a viable alternative to the WCUB equation [19] or the finite volume gas-kinetic scheme [23–25] for the simulation of aeroacoustic problems. An attempt to develop a modified $f^{eq}$ and apply it to DAS is therefore carried out. It is clear that the objective is to derive a modified $f^{eq}$ and its lattice counterpart that would allow the ideal gas law for diatomic gas and the Euler equations to be recovered correctly without having to invoke the $M \ll 1$ assumption. After all, the Euler equations have no $M$ limitations because $M$ simply does not appear in the normalized equations [18]. To derive a correct $\gamma$ for air, an alternative definition of the total energy under a proposed simplified gas particle model for diatomic gas is suggested. Thus formulated, the derived continuous $f^{eq}$ is a modified Maxwellian distribution plus other terms which are obtained by stipulating the contribution of the different internal degrees of freedom. The

constraints used to derive the modified $f^{eq}$ are the physical laws, i.e., the acoustic scaling form of the Euler equations, the ideal gas law, and the well-known equipartition theorem. A corresponding discrete $f^{eq}$ is also derived for the development of a finite difference lattice Boltzmann scheme. A high-order (at least sixth order) scheme with a two-dimensional nine-velocity (D2Q9) lattice model is used to solve the MBE, and the results are compared with direct numerical simulation (DNS) solutions of the benchmark two-dimensional (2-D) aeroacoustic problems. It is shown that only nine lattice vectors are required to obtain solutions of these aeroacoustic problems and the accuracy is just as good as, if not better than, the DNS solutions and those previously obtained by Li et al. [14,15], Kam et al. [16], and Li [31] using a D2Q13 velocity lattice.

## II. Recovery of Ideal Gas Law and Euler Equations

The starting point of the present analysis is the MBE with the BGK model invoked for the collision term. As a first attempt, the recovery of the ideal gas law and the acoustic scaling form of the Euler equations is attempted through the derivation of a modified $f^{eq}$. Thereafter, the methodology is extended to derive a lattice $f^{eq}$, so that it can be used to facilitate the numerical solution of the MBE. The BGK-type MBE is given by

$$\frac{\partial \hat{f}}{\partial \hat{t}} + \hat{\boldsymbol{\xi}} \cdot \nabla_{\hat{x}} \hat{f} = -\frac{1}{\hat{\tau}} (\hat{f} - \hat{f}^{eq}) \tag{1}$$

where the hat is used to denote dimensional quantities. To recover the acoustic scaling form of the Euler equations [18], Eq. (1) is made dimensionless by choosing the following characteristic parameters: $L = x_o/Kn$ as length, $c_r$ as velocity, $\tau_o$ as time, $\rho_r$ as density, $c_r^2/C_{pr}$ as temperature because this normalization would guarantee the recovery of the acoustic scaling form of the Euler equations [18]. The dimensionless variables are represented by symbols without the hat and they are given as

$$\begin{gathered} x = \frac{\hat{\mathbf{x}}}{x_o/Kn} = \frac{\hat{\mathbf{x}}}{L}, \qquad t = \frac{\hat{t}}{\tau_o/Kn} = \frac{\hat{t}}{L/c_r}, \qquad \tau = \frac{\hat{\tau}}{\tau_o} \\ p = \frac{\hat{\mathbf{p}}}{\rho_r c_r^2} \qquad \rho = \frac{\hat{\rho}}{\rho_r}, \qquad e = \frac{\hat{e}}{c_r^2}, \qquad \mathbf{u}, \boldsymbol{\xi} = \frac{\hat{\mathbf{u}}, \hat{\boldsymbol{\xi}}}{c_r} \\ T = \frac{\hat{T}}{c_r^2/C_{pr}} \qquad \theta = \frac{\hat{\theta}}{c_r^2}, \qquad f, f^{eq} = \frac{\hat{f}, \hat{f}^{eq}}{\rho_r/c_r^D} \\ f^{(n)} = \frac{\hat{f}^{(n)}}{\rho_r Kn^n/c_r^D}, \qquad n \geq 0 \end{gathered} \tag{2}$$

where boldface letters are used to denote vectors. Expanding $x_i$ (another form of writing $\mathbf{x}$), $t$, and $f$ in terms of $Kn$, the following expressions are obtained:

$$x_i = x_i^{(1)} + Kn x_i^{(2)} + \mathcal{O}(Kn^2) \tag{3a}$$

$$t = t^{(1)} + Kn t^{(2)} + \mathcal{O}(Kn^2) \tag{3b}$$

$$f = f^{(0)} + Kn f^{(1)} + Kn^2 f^{(2)} + \mathcal{O}(Kn^3) \tag{3c}$$

$$\frac{\partial}{\partial t} = \frac{\partial}{\partial t^{(1)}} + Kn \frac{\partial}{\partial t^{(2)}} \tag{3d}$$

$$\frac{\partial}{\partial x_i} = \frac{\partial}{\partial x_i^{(1)}} \tag{3e}$$

Collecting same order terms to $\mathcal{O}(Kn^2)$ gives the following three equations for the $f$s

$$f^{(0)} = f^{eq} \quad \text{to } \mathcal{O}(Kn^0) \tag{4}$$

$$\frac{\partial f^{(0)}}{\partial t^{(1)}} + \boldsymbol{\xi} \cdot \nabla_{x^{(1)}} f^{(0)} = -\frac{f^{(1)}}{\tau} \quad \text{to } \mathcal{O}(Kn^1) \tag{5}$$

$$\frac{\partial f^{(1)}}{\partial t^{(1)}} + \frac{\partial f^{(0)}}{\partial t^{(2)}} + \boldsymbol{\xi} \cdot \nabla_{x^{(1)}} f^{(1)} = -\frac{f^{(2)}}{\tau} \quad \text{to } \mathcal{O}(Kn^2) \tag{6}$$

This set of equations is solved to determine $f^{eq}$, $f^{(1)}$, $f^{(2)}$, etc., under certain macroscopic constraints to be specified. It should be pointed out that, to derive the Euler equations, only Eqs. (4) and (5) are required. Conventional thinking is that the NS equations and the fluid transport coefficients would require the consideration of Eq. (6).

### A. Ideal Gas Law and Macroscopic Constraints

The macroscopic constraints are specified by the recovery of the mass $\rho$, linear momentum $\rho\mathbf{u}$, and internal energy $e$. To recover $\gamma$ correctly, Li et al. [14] have shown that, in addition to $D_T$, $D_R$ also has to be considered in the energy model for $e_t$, the total internal energy. Therefore, the constraints are given by

$$\rho = \int f^{eq} \, d\boldsymbol{\xi} \tag{7}$$

$$\rho u_i = \int f^{eq} \xi_i \, d\boldsymbol{\xi} \tag{8}$$

$$\rho e_t = \rho e + \frac{1}{2}\rho |\mathbf{u}|^2 = \frac{D_T + D_R}{D} \int \frac{1}{2} f^{eq} |\boldsymbol{\xi}|^2 d\boldsymbol{\xi} \tag{9}$$

where the integral is evaluated over the whole velocity space. Defining $K = D_T + D_R - D$ as the number of internal degrees of freedom, Eq. (9) can be rewritten as

$$\begin{aligned} \rho e_t = \rho e + \frac{1}{2}\rho |\mathbf{u}|^2 &= \frac{D_T + D_R}{D} \int \frac{1}{2} f^{eq} |\boldsymbol{\xi}|^2 d\boldsymbol{\xi} \\ &= \int \frac{1}{2} f^{eq} |\boldsymbol{\xi} - \mathbf{u}|^2 d\boldsymbol{\xi} + \frac{K}{D} \int \frac{1}{2} f^{eq} |\boldsymbol{\xi}|^2 d\boldsymbol{\xi} + \frac{1}{2}\rho |\mathbf{u}|^2 \end{aligned} \tag{10}$$

where $(\boldsymbol{\xi} - \mathbf{u})$ is the peculiar velocity of a particle. The first term on the right-hand side of Eq. (10) is $\rho e$ and accounts for the translational motion of the particle, whereas the second term accounts for the rotational motion, and the third term represents the kinetic energy of the flow. This energy model is different from that assumed in the BGK model. In the following, it is shown that the second term in Eq. (10) is sufficient to allow the ideal gas law for a diatomic gas to be recovered and hence a correct estimate of $c$. Higher-order terms $f^{(n)}$ are given by

$$\int f^{(n)} \, d\boldsymbol{\xi} = 0 \tag{11a}$$

$$\int f^{(n)} \boldsymbol{\xi} \, d\boldsymbol{\xi} = 0 \tag{11b}$$

$$\frac{D_T + D_R}{D} \int \frac{1}{2} f^{(n)} |\boldsymbol{\xi}|^2 \, d\boldsymbol{\xi} = 0 \quad \text{for all } n \geq 1 \tag{11c}$$

If the ideal gas law were to be recovered identically, this requires that $p = \rho\theta$, and the equipartition theorem then gives

$$e = \frac{D_T + D_R}{2}\theta = \frac{\theta}{\gamma - 1} \quad \text{where } \gamma = \frac{D_T + D_R + 2}{D_T + D_R} \tag{12}$$

This leads to a correct expression for $e$ and an expression for $\gamma$ that does not depend on $D$. Therefore, $\gamma = 1.4$ is recovered exactly for any $D$ because $D_T = 3$ and $D_R = 2$, and $c^2 = \gamma\theta$ is calculated correctly once $\theta$ is known. The next step is to recover the set of Euler

equations and to identify constraints for the determination of a continuous $f^{eq}$.

### B. Recovery of Euler Equations

The continuity equation can be derived from the integral of Eq. (5) by first setting $f^{(0)} = f^{eq}$, the result (after setting $t = t^{(1)}$ and $x_j = x_j^{(1)}$) is

$$\int\left[\frac{\partial f^{eq}}{\partial t} + \frac{\partial}{\partial x_j}(\xi_j f^{eq}) = -\frac{f^{(1)}}{\tau}\right]d\boldsymbol{\xi} \Rightarrow \frac{\partial \rho}{\partial t} + \frac{\partial}{\partial x_j}(\rho u_j) = 0 \quad (13)$$

which yields the correct continuity equation without any restrictions.

Similarly, the momentum equation can be derived from the integral of Eq. (5) by first multiplying it by $\xi_i$ to give

$$\int\left[\frac{\partial f^{eq}}{\partial t} + \frac{\partial}{\partial x_j}(\xi_j f^{eq}) = -\frac{f^{(1)}}{\tau}\right]\xi_i\, d\boldsymbol{\xi}$$
$$\Rightarrow \frac{\partial(\rho u_i)}{\partial t} + \frac{\partial}{\partial x_j}(P_{ij} + \rho u_i u_j) = 0 \quad (14)$$

where $\int(\xi_i)(\xi_j)f^{eq}\, d\boldsymbol{\xi} = P_{ij} + \rho u_i u_j$ has been assumed and implies that $P_{ij}$ can be written as $P_{ij} = \int(\xi_i - u_i)(\xi_j - u_j)f^{eq}\, d\boldsymbol{\xi}$. Because the definition of $P_{ij}$ has to include a component equal to the static pressure $p$ if the momentum equation is to be recovered correctly, $P_{ij} \neq 0$. Therefore, rewriting $P_{ij}$ as $P_{ij} = p\delta_{ij} + P'_{ij}$, an expression for $P'_{ij}$ is deduced

$$P'_{ij} = \int(\xi_i)(\xi_j)f^{eq}\, d\boldsymbol{\xi} - \rho u_i u_j - p\delta_{ij} \quad (15a)$$

where $P'_{ij}$ has to satisfy the constraint

$$\partial P'_{ij}/\partial x_j = 0 \quad (15b)$$

With the stipulations given in Eq. (15), the inviscid momentum equation is identically recovered from Eq. (15) as

$$\frac{\partial(\rho u_i)}{\partial t} + \frac{\partial}{\partial x_j}(\rho u_i u_j) = -\frac{\partial p}{\partial x_i} \quad (16)$$

It remains to determine $P'_{ij}$ which depends on $f^{eq}$. The final expression for $P'_{ij}$ has to satisfy Eq. (15) and other constraints, if any, necessary for the recovery of the energy equation.

The energy equation can be derived from the integral of Eq. (5) by first multiplying it by $(|\boldsymbol{\xi}|^2/2)[(D_T + D_R)/D]$ to give

$$\int\left[\frac{\partial f^{eq}}{\partial t} + \frac{\partial}{\partial x_j}(\xi_j f^{eq})\right.$$
$$\left. = -\frac{f^{(1)}}{\tau}\right]\frac{|\boldsymbol{\xi}|^2}{2}\left(\frac{D_T + D_R}{D}\right)d\boldsymbol{\xi} \Rightarrow \frac{\partial}{\partial t^{(1)}}\left(\rho e + \frac{1}{2}\rho|\mathbf{u}|^2\right)$$
$$+ \frac{D_T + D_R}{D}\frac{\partial}{\partial x_j}\left(Q_j + u_j\left\{\frac{1}{2}\rho|\mathbf{u}|^2 + \frac{1}{2}P_{kk}\right\} + u_k P_{jk}\right) = 0 \quad (17)$$

where

$$Q_j = \left[\int(\xi_j - u_j)|\boldsymbol{\xi} - \mathbf{u}|^2 f^{eq}\, d\boldsymbol{\xi}\right]/2$$

has been assumed. It then follows that

$$\frac{1}{2}\int(\xi_j)|\boldsymbol{\xi}|^2 f^{eq}\, d\boldsymbol{\xi} = Q_j + u_j\left(\frac{1}{2}\rho|\mathbf{u}|^2 + \frac{1}{2}P_{kk}\right) + u_k P_{jk} \quad (18)$$

With these simplifications, and making use of $p = \rho\theta = (\gamma - 1)\rho e$, $P_{ij} = p\delta_{ij} + P'_{ij}$, and Eq. (15b), the following equation for $e$ is obtained

$$\frac{\partial}{\partial t}\left(\rho e + \frac{1}{2}\rho|\mathbf{u}|^2\right) + \frac{\partial}{\partial x_j}\left[u_j\left(\rho e + p + \frac{1}{2}\rho|\mathbf{u}|^2\right)\right]$$
$$+ \frac{\partial}{\partial x_j}\left[\frac{D_T + D_R}{D}Q_j + \frac{D_T + D_R - D}{D}u_j\left(\frac{1}{2}\rho|\mathbf{u}|^2\right)\right.$$
$$+ \frac{D_T + D_R - D}{D}pu_j + \frac{D_T + D_R}{D}\frac{1}{2}u_j P'_{kk}$$
$$\left. + \frac{D_T + D_R}{D}u_k P'_{jk}\right] = 0 \Rightarrow \frac{\partial}{\partial t}\left(\rho e + \frac{1}{2}\rho|\mathbf{u}|^2\right)$$
$$+ \frac{\partial}{\partial x_j}\left[u_j\left(\rho e + p + \frac{1}{2}\rho|\mathbf{u}|^2\right)\right] + \frac{\partial}{\partial x_j}(Q'_j) = 0 \quad (19)$$

where all terms inside the square bracket of the last term in Eq. (19) have been replaced by $Q'_j$. The energy equation can be identically recovered if $\partial Q'_j/\partial x_j = 0$ or $Q'_j = 0$ is assumed. Later derivation of $f^{eq}$ supports the assumption $Q'_j = 0$, and this leads to

$$Q_j = -\left[\frac{D_T + D_R - D}{D_T + D_R}u_j\left(\frac{1}{2}\rho|\mathbf{u}|^2\right) + \frac{D_T + D_R - D}{D_T + D_R}pu_j\right.$$
$$\left. + \frac{1}{2}u_j P'_{kk} + u_k P'_{jk}\right] \quad (20)$$

which can be evaluated once $P'_{ij}$ is completely determined. It is now clear that a knowledge of $f^{eq}$ would allow $P'_{ij}$ to be evaluated or vice versa. The determination of $P'_{ij}$ is given by the solution of Eq. (15).

## III. Formulation of Continuous $f^{eq}$

The constraints on the determination of a continuous $f^{eq}$ are the definitions for mass, linear momentum, and internal energy, i.e., Eqs. (7–9), plus the constraints on $P'_{ij}$ which are given by Eqs. (15). The definition for $P'_{ij}$ leads to a definite value for $P'_{ii}$, but the individual elements of $P'_{ij}$ still need to be evaluated. This can be accomplished once $f^{eq}$ is known. For monatomic gas, $f^{eq}$ is given by the Maxwellian distribution function [7]. The objective here is to find a modified $f^{eq}$ for diatomic gas that could satisfy the constraints given by the definitions of $\rho$, $\rho\mathbf{u}$, $e$, $P'_{ij}$, and $Q_j$. Once this is accomplished, the Euler equations are identically recovered with no additional restrictions other than the continuum assumption.

### A. Continuous $f^{eq}$

To simplify the mathematics for the determination of $f^{eq}$, the approach adopted here is to assume an $f^{eq}$ guided by previous analytical work [19–21] and to solve for $P'_{ij}$. It is obvious that the leading term should be given by a modified Maxwellian, so that in the limit of a monatomic gas the BGK model for $f^{eq}$ is recovered. Other terms should make up the moments of $\boldsymbol{\xi}$ with unknown parameters that could be scalars, vectors, or tensors. These terms are necessary if energy effects given rise by particle–particle collisions, other than the translational mode, and external heat source were to be accounted for. Sufficient number of moments should be considered so that all elements of $P'_{ij}$ can be determined. The constraints are then used to determine the unknown parameters. This approach to determine $f^{eq}$ is by no means unique; the viability of the resulting $f^{eq}$ is tested against benchmark problems in aerodynamics and aeroacoustics. Thus determined, the $f^{eq}$, with $\alpha_o$ a scalar, $\alpha_j$, $a_j$, and $b_i$ vectors, $\beta_{mn}$ a second-order tensor, and $\eta$ an unknown parameter, can be written as

$$f^{eq} = \alpha_o \exp\left[-\eta\sum_{k=1}^{D}(\xi_k - b_k)^2\right] + \sum_{i=1}^{D}\alpha_i\xi_i \exp[-\eta|\boldsymbol{\xi}|^2]$$
$$+ \sum_{m,n=1}^{D}\beta_{mn}\xi_m\xi_n \exp[-\eta|\boldsymbol{\xi}|^2] + \sum_{j=1}^{D}a_j\xi_j|\boldsymbol{\xi}|^2 \exp[-\eta|\boldsymbol{\xi}|^2] \quad (21)$$

The constraints given by Eqs. (7–9), (15a), and (20) for $\rho$, $\rho\mathbf{u}$, $e$, $P'_{ij}$, and $Q_j$ lead to the following equations for $\alpha_o$, $\alpha_j$, $a_j$, $b_i$, and $\beta_{mn}$, i.e.,

$$\rho = \left(\alpha_o + \sum_m^D \frac{\beta_{mm}}{2\eta}\right)\sqrt{\frac{\pi}{\eta}}^D \tag{22a}$$

$$\rho u_j = \left[\alpha_o b_j + \frac{\alpha_j}{2\eta} + \frac{(D+2)a_j}{4\eta^2}\right]\sqrt{\frac{\pi}{\eta}}^D \tag{22b}$$

$$\frac{2D}{D_T + D_R}\left(\rho e + \frac{1}{2}\rho|\mathbf{u}|^2\right) = \frac{\rho D}{2\eta} + \sum_k^D \alpha_o b_k^2 \sqrt{\frac{\pi}{\eta}}^D + \sum_m^D \frac{\beta_{mm}}{2\eta^2}\sqrt{\frac{\pi}{\eta}}^D \tag{22c}$$

$$\rho u_i u_j + p\delta_{ij} + P'_{ij} = \frac{\rho\delta_{ij}}{2\eta} + \alpha_o b_i b_j \sqrt{\frac{\pi}{\eta}}^D + \frac{\beta_{ij} + \beta_{ji}}{4\eta^2}\sqrt{\frac{\pi}{\eta}}^D \tag{22d}$$

$$\left(\frac{D}{2} + \frac{D}{D_T + D_R}\right)p u_j + \frac{D}{D_T + D_R}\frac{1}{2}\rho|\mathbf{u}|^2 u_j = \left(1 + \frac{D}{2}\right)\frac{\rho u_j}{2\eta} + \frac{\alpha_o b_j}{2}\sum_k^D b_k^2 \sqrt{\frac{\pi}{\eta}}^D + \frac{a_j}{8\eta^3}(D+2)\sqrt{\frac{\pi}{\eta}}^D \tag{22e}$$

From Eq. (22d), it is obvious that $\eta$ can be determined by assuming $p = \rho/2\eta$. Because the state equation for diatomic gas is given by $p = \rho\theta$, $\eta$ is evaluated to be $\eta = 1/2\theta$. It now remains to solve $P'_{ij}$ and determine $\alpha_o$, $\alpha_j$, $a_j$, $b_i$, and $\beta_{mn}$ introduced in Eq. (21).

### B. Solution of $P'_{ij}$ for Three-Dimensional Flow

Before proceeding to determine $\alpha_o$, $\alpha_j$, $a_j$, $b_i$, and $\beta_{mn}$, it is necessary to solve for $P'_{ij}$, which can be carried out by referring to the constraints given in Eq. (15). For the 3-D case and using Cartesian tensor notation, the $\partial P'_{ij}/\partial x_j = 0$ constraint in Eq. (15b) gives

$$\frac{\partial P'_{11}}{\partial x} + \frac{\partial P'_{12}}{\partial y} + \frac{\partial P'_{13}}{\partial z} = 0 \tag{23a}$$

$$\frac{\partial P'_{21}}{\partial x} + \frac{\partial P'_{22}}{\partial y} + \frac{\partial P'_{23}}{\partial z} = 0 \tag{23b}$$

$$\frac{\partial P'_{31}}{\partial x} + \frac{\partial P'_{32}}{\partial y} + \frac{\partial P'_{33}}{\partial z} = 0 \tag{23c}$$

According to Eq. (15a), the second-order tensor $P'_{ij}$ is symmetric and, because $P'_{ii}$ is the trace of $P'_{ij}$, it can be determined from Eq. (15a). The resulting expression is given by

$$\sum_{i=1}^D P'_{ii} = \frac{D - (D_T + D_R)}{D_T + D_R}\rho|\mathbf{u}|^2 \tag{24}$$

Taking the derivative of Eq. (23a) with respect to $y$ and $z$, that of Eq. (23b) with respect to $x$ and $z$, and that of Eq. (23c) with respect to $x$ and $y$, and then summing them up and invoking Eq. (24), the following equation is obtained:

$$\frac{\partial^3}{\partial x\partial y\partial z}\left[\frac{D - (D_T + D_R)}{D_T + D_R}\rho|\mathbf{u}|^2\right] + \frac{\partial}{\partial z}\left(\frac{\partial^2}{\partial x^2} + \frac{\partial^2}{\partial y^2}\right)P'_{12} + \frac{\partial}{\partial y}\left(\frac{\partial^2}{\partial x^2} + \frac{\partial^2}{\partial z^2}\right)P'_{13} + \frac{\partial}{\partial x}\left(\frac{\partial^2}{\partial y^2} + \frac{\partial^2}{\partial z^2}\right)P'_{23} = 0 \tag{25}$$

At this point, there are six unknowns, $P'_{11}, P'_{22}, P'_{33}, P'_{12}, P'_{13}, P'_{23}$, and only four equations, (23a–23c) and (24), therefore, there is freedom to make further simplifications. As a guide, consider the 2-D case. It can be easily shown that

$$\frac{\partial^2}{\partial x\partial y}\left[\frac{D - (D_T + D_R)}{(D_T + D_R)}\rho|\mathbf{u}|^2\right] + \left(\frac{\partial^2}{\partial x^2} + \frac{\partial^2}{\partial y^2}\right)P'_{12} = 0 \tag{26}$$

Analogously, the following isotropic assumption can be made for the 3-D case, such that

$$\frac{\partial^2}{\partial x\partial y}\left[\frac{D - (D_T + D_R)}{3(D_T + D_R)}\rho|\mathbf{u}|^2\right] + \left(\frac{\partial^2}{\partial x^2} + \frac{\partial^2}{\partial y^2}\right)P'_{12} = 0 \tag{27a}$$

$$\frac{\partial^2}{\partial x\partial z}\left[\frac{D - (D_T + D_R)}{3(D_T + D_R)}\rho|\mathbf{u}|^2\right] + \left(\frac{\partial^2}{\partial x^2} + \frac{\partial^2}{\partial z^2}\right)P'_{13} = 0 \tag{27b}$$

This choice is not unique either. Presumably, the isotropic assumption could be made for $P'_{12}$ and $P'_{23}$ or $P'_{13}$ and $P'_{23}$. Substituting Eqs. (27a) and (27b) into Eq. (25), an equation for $P'_{23}$ is obtained, i.e.,

$$\frac{\partial^3}{\partial x\partial y\partial z}\left[\frac{D - (D_T + D_R)}{3(D_T + D_R)}\rho|\mathbf{u}|^2\right] + \frac{\partial}{\partial x}\left(\frac{\partial^2}{\partial y^2} + \frac{\partial^2}{\partial z^2}\right)P'_{23} = 0 \tag{28}$$

With this equation, a complete set of equations for the determination of $P'_{ij}$ is now available.

Solving the Poisson equations given by Eqs. (27a), (27b), and (28), solutions for $P'_{12}$, $P'_{13}$, $P'_{23}$ are obtained. From Eqs. (23a–23c), the solutions for $P'_{11}$, $P'_{22}$, $P'_{33}$ can be deduced. One possible solution set for $P'_{ij}$ can now be written for an infinite domain $\mathbf{R}^D$ $(-\infty < x_i < \infty)$ as

$$P'_{ij} = \frac{1}{2\pi}\int_{-\infty}^{\infty}\int_{-\infty}^{\infty} f(x'_i, x'_j)\,\ell_n \frac{1}{\sqrt{(x_i - x'_i)^2 + (x_j - x'_j)^2}}\,\mathrm{d}x'_i\,\mathrm{d}x'_j \quad \text{for } i \neq j \tag{29a}$$

$$P'_{ij} = -\int \sum_{k\neq i}^D \frac{\partial P'_{ik}}{\partial x_k}\,\mathrm{d}x_i \quad \text{for } i = j \tag{29b}$$

where

$$f(x'_i, x'_j) = \frac{D - (D_T + D_R)}{D_o(D_T + D_R)}\frac{\partial^2\rho|\mathbf{u}|^2}{\partial x'_i\partial x'_j}$$

with $D_o = 1$ for 2-D flow and $D_o = 3$ for 3-D flow. Therefore, solutions for the 2-D and 3-D cases can be easily written from Eq. (29).

Once the solution for $P'_{ij}$ has been obtained, the parameters $\alpha_o$, $\alpha_j$, $a_j$, $b_i$, and $\beta_{mn}$ can be determined from Eqs. (22a–22e). The result with $D = 2$ or 3 is

$$\alpha_o = \frac{\rho}{\sqrt{2\pi\theta^D}} - \frac{D - (D_T + D_R)}{(D_T + D_R)\theta\sqrt{2\pi\theta^D}}\frac{1}{2}\rho|\mathbf{u}|^2 \tag{30a}$$

$$\alpha_j = \frac{1}{\theta}\left[\frac{\rho u_j}{\sqrt{2\pi\theta^D}} - \alpha_o b_j - (D+2)\theta^2 a_j\right] \tag{30b}$$

$$a_j = \frac{1}{(D+2)\theta^3\sqrt{2\pi\theta^D}}\left[u_j p\left\{\frac{D - (D_T + D_R)}{(D_T + D_R)}\right\} - \frac{b_j}{2}\rho|\mathbf{u}|^2 + \frac{D}{(D_T + D_R)}u_j\frac{1}{2}\rho|\mathbf{u}|^2\right] \tag{30c}$$

$$b_i = \frac{\pm u_i}{\sqrt{1-[D-(D_T+D_R)/(D_T+D_R)\theta](1/2)|\mathbf{u}|^2}} \tag{30d}$$

$$\beta_{ij} = \frac{P'_{ij}}{2\theta^2\sqrt{2\pi\theta^D}} \tag{30e}$$

Note that, in the derivation of a modified $f^{eq}$, no stipulation has been imposed on $\tau$ in the BGK model given in Eq. (1). This suggests that the MBE thus modified is not restricted to a particular $\tau$ and its solution might not require adjustment to be made to $\tau$. The $f^{eq}$ thus derived allows the acoustic scaling form of the Euler equations to be recovered with no additional assumption other than the dense gas assumption ($Kn \ll 1$). Further note that all parameters will either reduce to the BGK model identically or become zero for the monatomic gas case. For monatomic gas, $D_T = 3$, $D_R = 0$, and $P'_{ij} = 0$ for $i, j = 1, \ldots, D$. If the positive sign in Eq. (30d) is chosen, then $b_i = u_i$, $\alpha_o = \rho/\sqrt{2\pi\theta^D}$, $\alpha_i = a_i = 0$, and $\beta_{ij} = 0$ for $i, j = 1, \ldots, D$. It then follows $f^{eq}$, as given in Eq. (21), reduces to a Maxwellian distribution function and the original BGK model is fully recovered.

## IV. Lattice $f^{eq}$ and Lattice Boltzmann Method Simulation

The improved MBE is still a linear scalar equation with all nonlinear particle collision effects modeled in the modified $f^{eq}$. It is anticipated that the modified $f^{eq}$ could more accurately reflect the physics of the aerodynamic–aeroacoustic interaction. The scalar equation is very amenable to numerical treatment and is not limited to the velocity lattice method alone. Other finite difference schemes, such as those proposed by Xu and Prendergast [23–25], could be used to solve the equation numerically.

In the present study, the LBM is used to solve Eq. (1) with the modified $f^{eq}$ given by Eq. (21), and the results are compared with two benchmark aeroacoustic problems previously obtained by Li et al. [14] and Li [31] using both LBM and DNS schemes. The purpose of this comparison is to show that a more general $f^{eq}$ would allow the aeroacoustic disturbances to be evaluated accurately even when a coarser lattice is used. By way of this comparison, the importance of correctly modeling the nonlinear physics of the collision processes of diatomic gas in $f^{eq}$ is demonstrated as well as the overall validity of the modified BGK model for the BE. The use of LBM to solve the MBE requires a corresponding lattice $f^{eq}$. In this section, the lattice $f^{eq}$ is derived and the associated parameters are determined by invoking the constraints given in Eqs. (22a–22e).

### A. Lattice $f^{eq}$

Just as in the case of the continuous $f^{eq}$, the lattice $f^{eq}$ also has to lead to the Euler equations exactly without having to assume $M \ll 1$. In the past, derivation of a lattice $f^{eq}$ relied on a Taylor expansion of the Maxwellian distribution function [8]. The expansion is usually made in terms of $\boldsymbol{\xi} \cdot \mathbf{u}$ and terminated after the second or third order. The Taylor series is further assumed to be multiplied by weighting factors that are dependent on the assumed lattice model used to represent the discrete velocity space. These weighting factors are determined from the constraints used to recover the Euler or NS equation. Inherent in the Taylor expansion, in terms of $\boldsymbol{\xi} \cdot \mathbf{u}$, is the assumption that $M \ll 1$. Therefore, it is this expansion that renders the LBM not entirely valid for any $M$ [32]. If the present method were to be free of this assumption, another approach to derive a lattice $f^{eq}$ that does not depend on an expansion in terms of $\boldsymbol{\xi} \cdot \mathbf{u}$ has to be found. A parallel could be drawn from the approach of Philippi et al. [33]. Instead of expanding $f^{eq}$ in terms of $\boldsymbol{\xi} \cdot \mathbf{u}$, a polynomial series in $\boldsymbol{\xi}$ up to its second order could be assumed. Each term in the series is weighted by coefficients that could be scalars, vectors, or tensors depending on the nature of the term. With this understanding, derivation of the lattice $f^{eq}$ can now proceed forward.

Discretize the velocity space using the velocity lattice for a 2-D flow and the discrete form of Eq. (1) becomes

$$\frac{\partial f_\alpha}{\partial t} + \xi_\alpha \cdot \nabla_x f_\alpha = -\frac{1}{\tau Kn}(f_\alpha - f_\alpha^{eq}) \tag{31}$$

where $\alpha$ is the index for the lattice velocity. In anticipation that, at most, a D2Q13 model is required for accurate resolution of aeroacoustic problems, only the methodology for the derivation of a D2Q13 lattice $f_\alpha^{eq}$ is presented next. For such a model, the lattice velocity is given by

$$\xi_o = 0, \qquad \alpha = 0 \tag{32a}$$

$$\xi_\alpha = \sigma\{\cos[\pi(\alpha-1)/4], \quad \sin[\pi(\alpha-1)/4]\}, \qquad \alpha = 1, 3, 5, 7 \tag{32b}$$

$$\xi_\alpha = \sqrt{2}\sigma\{\cos[\pi(\alpha-1)/4], \quad \sin[\pi(\alpha-1)/4]\} \qquad \alpha = 2, 4, 6, 8 \tag{32c}$$

$$\xi_\alpha = 2\sigma\{\cos[\pi(\alpha-1)/2], \quad \sin[\pi(\alpha-1)/2]\} \qquad \alpha = 9, 10, 11, 12 \tag{32d}$$

where $\sigma$ is a parameter to be specified later. A polynomial series in the particle velocity $\xi_\alpha$ is assumed for the discretized form of $f_\alpha^{eq}$. To the second order, it can be written in 2-D Cartesian form as

$$f_\alpha^{eq} = A_\alpha + \xi_{\alpha x} Ax_\alpha + \xi_{\alpha y} Ay_\alpha + \xi_{\alpha x}^2 Bxx_\alpha + \xi_{\alpha y}^2 Byy_\alpha + \xi_{\alpha x}\xi_{\alpha y} Bxy_\alpha \tag{33}$$

where the coefficients $A_\alpha$, $Ax_\alpha$, $Bxx_\alpha$, etc., could be scalars, vectors, or tensors. The constraints used to recover the Euler equations in discrete form for 2-D flows are obtained from Eqs. (22a–22e), and the resulting equations are used to determine $A_\alpha$, $Ax_\alpha$, $Bxx_\alpha$, etc. Note that this will give rise to nine equations. However, one equation is redundant because it is a duplicate of the kinetic energy equation. Consequently, only eight equations remain. The eight equations have as unknowns the elements of $P'_{ij}$, which for a 2-D flow are reduced to $P'_{xx}$, $P'_{xy}$, and $P'_{yy}$; their values are given by solving Eqs. (23a), (23b), and (26).

If the coefficients having the same "energy shell" of the lattice velocities are assumed to be the same, the number of unknowns resulting from the coefficients $A_\alpha$, $Ax_\alpha$, $Bxx_\alpha$, etc., are reduced to 19 for the D2Q13 case and 13 for the D2Q9 case. Because only eight constraints are available for the determination of these coefficients, there is certain flexibility and assumptions can be made to facilitate solution of the eight equations. As a first attempt, 11 (or five) coefficients can be assumed zero. Because simple algebra is involved, details of this derivation are not shown; therefore, only the results for the coefficients in Eq. (33) are given. One possible set of solutions is

$$A_o = \rho - \frac{2p}{\sigma^2} - (\gamma-1)\frac{\rho|\mathbf{u}|^2}{\sigma^2}, \qquad A_1 = A_2 = A_9 = 0 \tag{34a}$$

$$Ax_1 = \frac{2}{3}\frac{\rho u}{\sigma^2} - \frac{1}{3}\frac{\gamma p u}{\sigma^4} - (\gamma-1)\frac{1}{6}\frac{\rho|\mathbf{u}|^2 u}{\sigma^4}, \qquad Ax_2 = 0 \tag{34b}$$

$$Ax_9 = -\frac{1}{24}\frac{\rho u}{\sigma^2} + \frac{1}{12}\frac{\gamma p u}{\sigma^4} + (\gamma-1)\frac{1}{24}\frac{\rho|\mathbf{u}|^2 u}{\sigma^4} \tag{34c}$$

$$Ay_1 = \frac{2}{3}\frac{\rho v}{\sigma^2} - \frac{1}{3}\frac{\gamma p v}{\sigma^4} - (\gamma-1)\frac{1}{6}\frac{\rho|\mathbf{u}|^2 v}{\sigma^4}, \qquad Ay_2 = 0 \tag{34d}$$

$$Ay_9 = -\frac{1}{24}\frac{\rho v}{\sigma^2} + \frac{1}{12}\frac{\gamma p v}{\sigma^4} + (\gamma - 1)\frac{1}{24}\frac{\rho|\mathbf{u}|^2 v}{\sigma^4} \tag{34e}$$

$$Bxx_1 = \frac{1}{2\sigma^4}(p + \rho u^2 + P'_{xx}), \qquad Bxx_2 = Bxx_9 = 0 \tag{34f}$$

$$Byy_1 = \frac{1}{2\sigma^4}(p + \rho v^2 + P'_{yy}), \qquad Byy_2 = Byy_9 = 0 \tag{d34g}$$

$$Bxy_2 = \frac{1}{4\sigma^4}(\rho uv + P'_{xy}), \qquad Bxy_1 = Bxy_9 = 0 \tag{34h}$$

For a D2Q9 model, the velocity lattices are as defined in Eqs. (32a–32c) and the lattice $f^{\text{eq}}$ is again given by Eq. (33). The coefficients in the lattice $f^{\text{eq}}$ can be similarly determined. Finally, it should be noted that the solution thus obtained is not unique. Therefore, numerical results obtained from the discretized MBE have to be validated against analytical results or DNS solutions of aeroacoustic problems.

### B. Improved Lattice Boltzmann Method Simulation

The discrete Boltzmann equation [Eq. (31)] can be viewed as a system of inhomogeneous hyperbolic equations, and any standard finite difference scheme can be used to solve it. Traditionally, the lattice Boltzmann method refers to a particular discretization of Eq. (31), with second-order accuracy in both spatial and temporal dimensions. This simple formulation is called the lattice Boltzmann equation (LBE) [34]. Because this scheme is only second-order accurate, it is not suitable for DAS which requires high-order accuracy. It is precisely for this reason that a higher-order scheme is used in the present study. In the present numerical scheme, the term on the right-hand side of Eq. (31) is evaluated locally at every time step, whereas the second term on the left-hand side of Eq. (31) is estimated using a sixth-order finite difference scheme similar to that proposed by Lele [18]. A second-order Runge–Kutta time-marching scheme is used to calculate the time-dependent term in Eq. (31). Because the present scheme does not use the specific discretization for LBE, strictly speaking, it is actually not an LBM scheme. Rather, according to the terminology of Cao et al. [35], it is a finite difference scheme for the lattice Boltzmann equation or a finite-difference-based lattice Boltzmann method [36]. However, for the sake of simplicity, the present numerical scheme will still be denoted as LBM.

Details of the present numerical scheme used to solve the discretized MBE are given in Li [31]; therefore, only the salient points are repeated here. Li et al. [14,15] and Kam et al. [16] used a computational domain of $22 \times 22$ with a grid size of $0.05 \times 0.05$ to carry out their LBM and DNS simulations. To compare current calculations with previous results [14], the same computational domain and grid size is used in the present study. The relaxation time $\tau$ in Eq. (31) could be specified as follows. In the present formulation, $\tau$ and $Kn$ appear together as $\tau Kn$ in Eq. (31), thus implying that $\tau$ and $Kn$ need not be specified separately. Because $\tau$ is of $\mathcal{O}(1)$ and $Kn$ is assumed to be very small (on the order of $10^{-7}$ according to Chapman and Cowling [17]), the term $\tau Kn$ should be much smaller than one when compared to other terms in Eq. (31). In the present calculation, $\Delta t = \tau Kn = 10^{-5}$ is chosen, and this is sufficient to give results that are in excellent agreement with DNS. Furthermore, numerical instability was not encountered in all calculations carried out in this study, even without using any high-order filter.

Different nonreflecting boundary conditions have been tested and the absorbing boundary condition was found to give reliable and accurate results compared with those obtained from DNS simulations [16]. The absorbing region is chosen to be one, same as that specified by Kam et al. [16]. As for the damping coefficient, its choice varies from problem to problem. Again, the value chosen in [16] is used as the initial guess and it will be adjusted depending on the problem investigated. In the present study, a D2Q9 model is used instead of a D2Q13 one, because later calculations show that the coarser model is sufficient to give results with accuracy comparable to DNS simulations. This is evidence that the modified $f^{\text{eq}}$ with sufficient particle collision physics built in is more preferable than a finer lattice or the adoption of a multiple relaxation time [37,38].

Besides the nonreflecting boundary condition necessary for $f$, it should be noted that, in solving for the macroscopic properties using Eqs. (22a–22e) for the case of a 2-D flow, the tensor $P'_{ij}$ needs to be evaluated from Eqs. (23), (24), and (26). Therefore, boundary conditions are also required for all elements of $P'_{ij}$. As a first attempt, either the first or second derivative of $P'_{ij}$ is specified to be zero at all boundaries of the computational domain. As later calculations will show, setting the first derivatives to zero is sufficient for the aeroacoustic problems studied. Finally, an estimate of the magnitude of the lattice velocity $\sigma$ can be made. From Eq. (22c), and making use of $p = \rho\theta$, the following bounds can be deduced for the particle velocity $\xi_\alpha$, i.e.,

$$\begin{aligned}\min(|\xi_\alpha|^2)\sum_{\alpha=0}^{N} f_\alpha^{\text{eq}} &\le \frac{4}{D_T + D_R}\left(\rho e + \frac{1}{2}\rho|\mathbf{u}|^2\right) \\ &\le \max(|\xi_\alpha|^2)\sum_{\alpha=0}^{N} f_\alpha^{\text{eq}}\end{aligned} \tag{35}$$

Making use of the macroscopic constraints, Eqs. (22a) and (32b), the magnitude of $\sigma$ can be determined as $\sigma^2 = |\xi_\alpha|^2$, or explicitly as

$$\sigma = |\xi_\alpha| = \left[\frac{2p_\infty}{\rho_\infty} + \frac{2}{D_T + D_R}(u_\infty^2 + v_\infty^2)\right]^{1/2} \tag{36}$$

for $\alpha = 1$, 3, 5, and 7 only.

## V. Results and Discussion

The improved LBM is validated against two benchmark aeroacoustic problems that have been attempted by Li et al. [14] and Li [31]. The problems are the propagation of a circular pulse in a quiescent fluid and the propagation and interaction of three pulses in a uniform stream. These two problems are chosen because they are able to test the ability of the improved LBM to replicate the isotropic behavior of propagation and the interaction between a vortex, a pressure, and an entropy pulse in a uniform stream.

In view of the credibility and accuracy of the DNS scheme, it is used in the present study as a benchmark to assess the improved LBM simulations. The DNS calculations are carried out by solving Eqs. (13), (16), and (19) using a five-point, sixth-order compact finite difference scheme suggested by Lele [2] to obtain the spatial derivative, and an explicit fourth-order Runge–Kutta scheme for time marching. The high-order filtering of Visbal and Gaitonde [39] was applied to every final stage of the Runge–Kutta scheme to suppress numerical instabilities due to spatial differencing. Again, a domain size of $22 \times 22$ with grid size given by $0.05 \times 0.05$ was used. The effect of different nonreflecting boundary conditions has been investigated before and the absorbing boundary condition was found to give the best result [16]. The dimensionless width of the absorbing region is chosen to be one. Details of the DNS scheme and its solutions of specific aeroacoustic problems are given elsewhere [31]; therefore, they will not be repeated here.

The errors between the LBM and DNS solutions of a macroscopic variable $\mathbf{b}$ are expressed in terms of the $L_q$ integral norm, i.e.,

$$\|L_q(\mathbf{b})\| = \left[\frac{1}{N}\sum_{j=1}^{N}|\mathbf{b}_{\text{LBM},j} - \mathbf{b}_{\text{DNS},j}|^q\right]^{\frac{1}{q}} \tag{37a}$$

for any integer $q$, and its maximum

$$\|L_\infty(\mathbf{b})\| = \max_j |\mathbf{b}_{\mathrm{LBM},j} - \mathbf{b}_{\mathrm{DNS},j}| \tag{37b}$$

The results of the improved LBM are compared with DNS calculations and the error norms are deduced according to Eqs. (37a) and (37b). A comparison of these error norms with previously deduced results [14,31] is also made.

### A. Circular Pulse in Quiescent Fluid

The fluctuations created by an initial circular pulse in quiescent fluid would propagate equally in all directions. Because there is no dissipation, the pulse would remain circular in shape for all time. To test the ability of the improved LBM with a D2Q9 lattice to replicate the isotropic property of a circular pulse, it is used to simulate a circular pressure pulse located at $(x, y) = (0, 0)$ initially, and with distribution given by

$$\rho = \rho_\infty, \qquad u = 0, \qquad v = 0$$
$$p = p_\infty + \varepsilon \exp\left(-\ell_n 2 \times \frac{x^2 + y^2}{0.2^2}\right) \tag{38}$$

According to the acoustic scaling given in Eq. (2), $\rho_\infty = 1$ and $p_\infty = 1/\gamma$, whereas $\varepsilon$ is chosen to be $\varepsilon = 1 \times 10^{-4}$. For this problem, $\sigma$ is estimated from Eq. (36) and $\Delta t = 0.00001$ is chosen for the time step. Because the grid size is given by $\Delta x = \Delta y = 0.05$, the ratio $\Delta x/\Delta t = \Delta y/Dt = 5 \times 10^3$ is 100 times larger than that used in the DNS simulation. This ratio is not related to $c$ as some previous work on LBM suggested that it should. Computations are carried out in the $22 \times 22$ domain as well as in a smaller domain. In anticipation of the fact that the Mach number at upstream infinity is specified as $M_\infty = 0.9$ for the three-pulse case, the choice of this smaller domain cannot be too small; therefore, it is chosen to be $12 \times 12$ or slightly larger than one-quarter the size of the $22 \times 22$ domain. This is because the pulses would exit a smaller computational domain in a very short time for $M_\infty = 0.9$ and there is little left in the domain to see at $t = 1$. Because the absorbing region is chosen to be one, the actual computational domain is $20 \times 20$ and $10 \times 10$ rather than $22 \times 22$ and $12 \times 12$. It is found that the results within the region $8 \times 8$ of the two different calculations are essentially identical. Therefore, only the results of the small domain simulations are reported. The error norms as specified in Eqs. (37a) and (37b) are evaluated using the improved LBM results from the small domain calculations and the DNS simulation from the large $(22 \times 22)$ domain. They are listed in Table 1 for comparison. The $L_q$ and $L_\infty$ are comparable if not better than those obtained by Li [31] using a D2Q13 lattice model. This shows that a physically appropriate $f^{\mathrm{eq}}$ plays a more significant role than a finer lattice model.

The contours of $p$ and $u$ fluctuations are shown in Figs. 1a and 1b at $t = 2.5$ and $t = 5$, respectively. Results from the improved LBM simulations are shown in the top half of each panel, whereas the lower half depicts the corresponding results from the DNS calculations. Corresponding results of $p - p_\infty$ and $u - u_\infty$ along $y = 0$ are plotted in Figs. 2a and 2b. It can be seen that the pulse essentially remains circular as $t$ increases, thus implying the

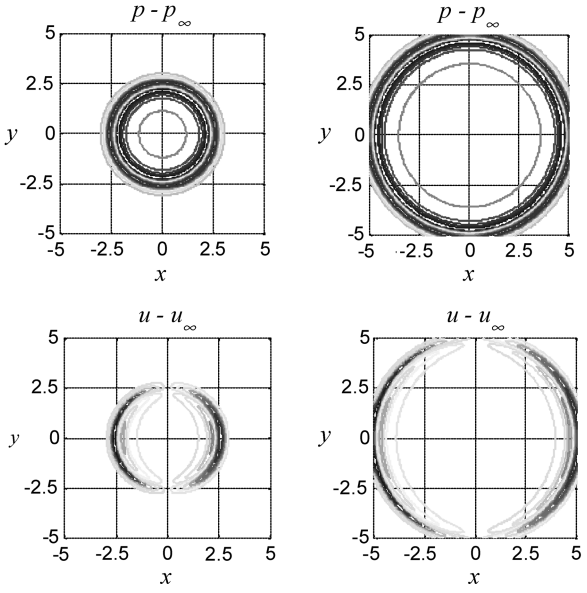


a) b)

**Fig. 1 Contour map of the pressure and $u$-velocity fluctuation at a) $t = 2.5$ and b) $t = 5.0$; lower half is DNS solution, top half is improved LBM solution. There are 16 equally distributed contour lines in each plot bounded by a maximum of 9.5830E − 06 and a minimum of −4.9660E − 06 for Fig. 1a; a maximum of 6.8663E − 06 and a minimum of −3.3495E − 06 for Fig. 1b.**

simulation using the improved LBM with a D2Q9 lattice is able to predict the isotropic behavior of the circular pulse. Furthermore, the improved LBM is sufficient to capture all details of the acoustic field as given by the DNS solution.

To assess the effect of $P'_{ij}$ on the improved LBM results, the contour plots of the three components of $P'_{ij}$ at $t = 2.5$ and $t = 5$ are shown in Figs. 3a and 3b, respectively. The top panel of these two figures shows $P'_{xy}$, whereas the middle and bottom panels show $P'_{xx}$ and $P'_{yy}$, respectively. The center of $P'_{ij}$ coincides with the center of the acoustic pressure pulse and is located at $x = 0$ and $y = 0$. Because there is no mean flow, the center does not move as $t$ increases. The $P'_{ij}$ elements are essentially symmetric about the $x$ and $y$ axis. This symmetry remains unchanged with increasing $t$. It can be seen that the maximum magnitude of the three elements of $P'_{ij}$ is very small, the largest is on the order of $10^{-11}$, and is about 3 orders of magnitude smaller than $L_q$ and $L_\infty$. The three elements of $P'_{ij}$ are essentially identically zero. The reason why they are zero is because $\sum P'_{ii}$ is essentially zero for the present problem where there is no mean flow, a consequence of Eq. (24). According to Eqs. (33) and (34), the three nonlinear terms on the right-hand side of Eq. (33) are reduced to functions of $p$ and $\rho\mathbf{u} \cdot \mathbf{u}$; consequently, $P'_{ij}$ has no effect on the calculation of $Bxx_1$, $Byy_1$, $Bxy_1$. This is an indication that the effect of $P'_{ij}$ on the calculated acoustic properties is insignificant; a consequence of the lack of nonlinear effects due to the interaction of

**Table 1 Error norms of improved LBM and DNS simulations of two aeroacoustic cases investigated**

| | | | | | | |
|---|---|---|---|---|---|---|
| | | | *Circular pulse in quiescent fluid* | | | |
| | $t = 2.5$ | | | $t = 5.0$ | | |
| Error norm | $L_\infty$ | $L_2$ | $L_1$ | $L_\infty$ | $L_2$ | $L_1$ |
| Pressure | 1.6249E − 08 | 2.6032E − 09 | 1.0302E − 09 | 2.1947E − 08 | 4.6028E − 09 | 2.2061E − 09 |
| Density | 2.6244E − 07 | 5.8839E − 09 | 1.3166E − 09 | 5.2212E − 07 | 1.1496E − 08 | 2.7932E − 09 |
| $u$ velocity | 1.5352E − 08 | 1.8364E − 09 | 6.3757E − 10 | 2.0673E − 08 | 3.2785E − 09 | 1.4106E − 09 |
| | | | *Three pulses in a uniform stream* | | | |
| | $t = 1.0$ | | | $t = 1.5$ | | |
| Error norm | $L_\infty$ | $L_2$ | $L_1$ | $L_\infty$ | $L_2$ | $L_1$ |
| Pressure | 1.3111E − 06 | 1.0608E − 07 | 2.9029E − 08 | 1.2679E − 06 | 1.2835E − 07 | 4.2244E − 08 |
| Density | 1.3113E − 06 | 1.0820E − 07 | 3.0902E − 08 | 1.2680E − 06 | 1.3197E − 07 | 4.5280E − 08 |
| $u$ velocity | 5.3208E − 07 | 3.8654E − 08 | 1.1463E − 08 | 7.9731E − 07 | 5.2193E − 08 | 1.8421E − 08 |

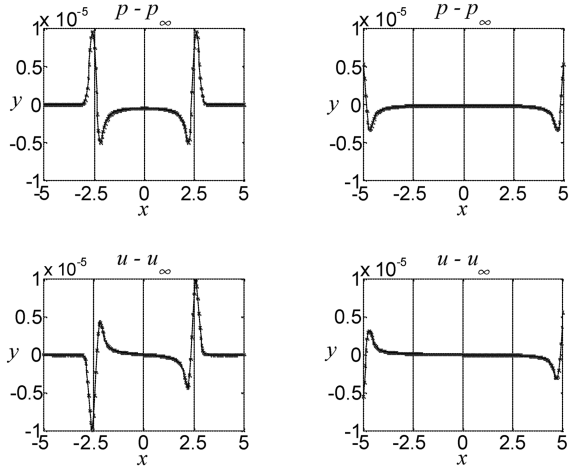


a) b)

**Fig. 2 Distributions of the pressure and $u$-velocity fluctuation along the $x$ axis at a) $t = 2.5$ and b) $t = 5.0$; straight line is DNS solution; x indicates improved LBM solution.**

aerodynamics and acoustics in the present problem. Therefore, the $P'_{ij}$ results suggest that they are a measure of the importance of this nonlinear interaction effect and are essentially zero for a linear aeroacoustic problem.

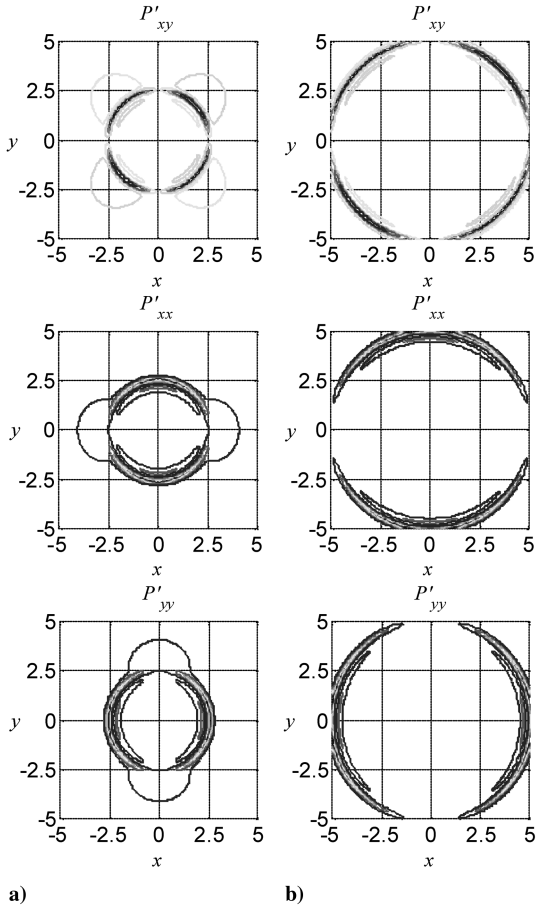


a) b)

**Fig. 3 Contour map of $P'_{xy}, P'_{xx}, P'_{yy}$ fluctuation distribution at a) $t = 2.5$ and b) $t = 5.0$; lower half is DNS result, top half is improved LBM result. There are eight equally distributed contour lines in each plot. The maximum and minimum bounds for Fig. 3a are 2.6064E − 11 and −2.6059E − 11, 4.5406E − 12 and −5.5179E − 11, 4.5442E − 12 and −5.5202E − 11; for Fig. 3b they are 1.3012E − 11 and −1.3010E − 11, 6.5680E − 13 and −2.8743E − 11, 7.4020E − 13 and −2.8758E − 11, respectively, for $P'_{xy}, P'_{xx}, P'_{yy}$.**

### B. Three Pulses in a Uniform Stream

The three-pulse interaction problem consists of a pressure, a vorticity, and an entropy pulse propagating in a uniform mean flow $u_\infty$. Basically, only the pressure pulse is propagating with speed $c$, the entropy pulse and the vortex pulse would move with $u_\infty$. The initial conditions are as given in Tam and Webb [3], i.e.,

$$\rho = \rho_\infty + \varepsilon_1 e^a + \varepsilon_2 e^b, \qquad p = p_\infty + \varepsilon_1 e^a \tag{39a}$$

$$u = u_\infty + \varepsilon_2 y e^b, \qquad v = v_\infty - \varepsilon_2 (x-1) e^b \tag{39b}$$

$$a = -\ln 2\left(\frac{(x+1)^2 + y^2}{0.2^2}\right), \qquad b = -\ln 2\left(\frac{(x-1)^2 + y^2}{0.4^2}\right) \tag{39c}$$

where $\varepsilon_1 = 0.0001$ and $\varepsilon_2 = 0.001$. The mean field has reference density, speed, and pressure given by $\rho_\infty = 1$, $u_\infty = 0.9$, $v_\infty = 0$, $p_\infty = 1/\gamma$. These initial conditions, except $M_\infty$, are identical to those specified in [14,16]. According to the acoustic scaling given in Eq. (2), $u_\infty$ is identical to $M_\infty$. To illustrate the ability of the present formulation to handle flows with high subsonic $M$, the choice $u_\infty = M_\infty = 0.9$ is specified. Smaller $M_\infty$ cases have also been calculated to ensure the applicability of the improved LBM for all subsonic $M_\infty$ tested. Initialization of the pressure pulse is carried out at $x = -1$, $y = 0$, whereas the entropy and the vorticity pulse is initialized at $x = 1$, $y = 0$. Again, $\sigma$ is estimated from Eq. (36), $\Delta t = 0.00001$ and $\Delta x = \Delta y = 0.05$ are specified. The ratio $\Delta x/\Delta t = \Delta y/\Delta t = 5 \times 10^3$ again has no relation to $c$. The computational domain is chosen to be $12 \times 12$ to avoid the exiting of the pulses from the computational boundary prematurely. The actual domain is $10 \times 10$ after the absorbing region is subtracted out. As before, the reference solution is given by the DNS solution in a $22 \times 22$ domain.

In the course of carrying out the simulation of this problem, it was found that just invoking the absorbing boundary condition at the inlet and outlet boundaries was not sufficient to suppress all disturbances arising from boundary reflection and truncation errors. As a result, very small background noises started to appear at the inlet boundary after a finite period of time. To prevent this reflected wave from propagating back into the computational domain, further treatment at the boundaries is necessary. Several boundary treatments were tried and it was found that the filtering treatment of Visbal and Gaitonde [39] gives the best result. Consequently, this filtering treatment was implemented after every time step, just as the case in the DNS calculation. The results thus obtained are free of reflected disturbances from the inlet and outlet boundaries.

In the calculation of Li et al. [14], the assumption of symmetry coefficients of the lattice requires $\mathbf{u}$ to be much smaller than $\boldsymbol{\xi}$. This assumption is also inherent in the Taylor expansion of the Maxwellian distribution made to derive the lattice $f^{\text{eq}}$. For a problem with a relatively large $u_\infty$, the validity of the Taylor expansion of the Maxwellian function is called into question. Consequently, $u_\infty$ was subtracted from $\mathbf{u}$ and $\boldsymbol{\xi}$ in the definition of the Maxwellian distribution function for this interaction problem. The present formulation is not bounded by the $M \ll 1$ assumption; hence, it is not necessary to invoke their treatment to $\mathbf{u}$ and $\boldsymbol{\xi}$. Therefore, a comparison between the present results and those obtained previously [14,16] will further illustrate the importance of not having to assume $M \ll 1$ in the formulation of the improved LBM.

The $p$ and $u$ contours at $t = 1$ and $t = 1.5$ are plotted in Figs. 4a and 4b. Again, the top half of each panel shows the improved LBM result, whereas the lower half depicts the DNS calculation. The distributions of $p - p_\infty$ and $u - u_\infty$ along the $x$ axis at $t = 1$ and $t = 1.5$ are shown in Figs. 5a and 5b, respectively, together with the analytical inviscid solution [3]. All three solutions are essentially identical. The calculated $L_q$ and $L_\infty$ are listed in Table 1 for comparison. Their values are on the order of $10^{-6}$ or smaller. Similar results are also obtained for cases with lower $M_\infty$ and the result for

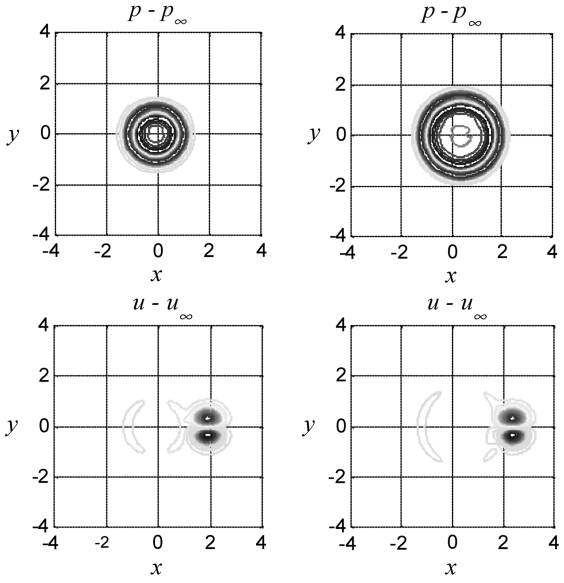


**Fig. 4 Contour map of the pressure and $u$-velocity fluctuation at a) $t = 1.0$ and b) $t = 1.5$; lower half is DNS solution, top half is improved LBM solution. There are 16 and 30 equally distributed contour lines in the pressure and velocity plot, respectively, and the (maximum, minimum) values of the pressure and $u$ velocity at $t = 1.0$ and $t = 1.5$ are (1.4619E − 05, −9.6695E − 06) for $p$ and (2.0576E − 04, −2.0582E − 04) for $u$; (1.2167E − 05, −7.2213E − 06) for $p$ and (2.0586E − 04, −2.0560E − 04) for $u$, respectively.**

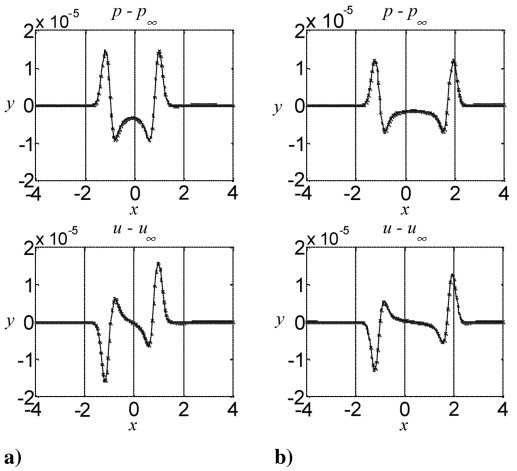


**Fig. 5 Distributions of the pressure and $u$-velocity fluctuation along $x$ axis at a) $t = 1.0$ and b) $t = 1.5$: straight line is DNS and analytical solution; x denotes improved LBM solution.**

the $M_\infty = 0.2$ case is in agreement with [16], but they are not shown for the reason of conciseness. Together, these results show that the improved LBM is a viable alternative to the DNS for this three-pulse problem.

The contour plots of the three elements of $P'_{ij}$ at $t = 1$ and $t = 1.5$ are shown in Figs. 6a and 6b, respectively. In each figure, the panels from top to bottom depict $P'_{xy}$, $P'_{xx}$, and $P'_{yy}$, respectively. The shape of the $P'_{xy}$ contour looks like a four-leaf clover (Oxalis Deppei), whereas those of $P'_{xx}$ and $P'_{yy}$ are like dumbbells. It can be seen that the maximum magnitude of the contours is about $10^{-1}$. In general, the magnitudes of the contours have increased significantly, a consequence of Eq. (24) where $u^2$ is on the order of one. This fully illustrates the nonlinear behavior resulting from the interaction of the mean flow with the pressure, vorticity, and entropy pulses. In other words, the modified $f^{eq}$ could sufficiently mimic the nonlinear particle–particle interaction to reflect the nonlinear aerodynamic-

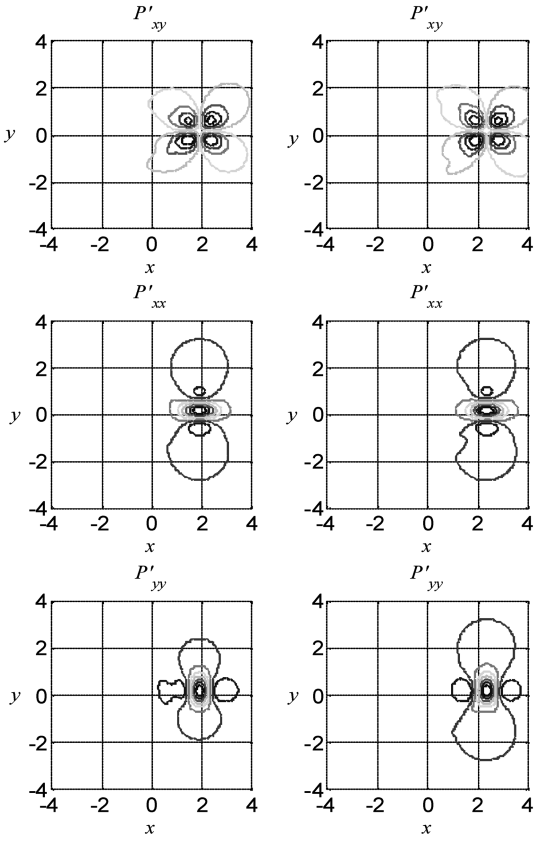


**Fig. 6 Contour map of $P'_{xy}$, $P'_{xx}$, $P'_{yy}$ fluctuation distribution at a) $t = 2.5$ and b) $t = 5.0$; lower half is DNS result, top half is improved LBM result. There are eight equally distributed contour lines in each plot. The (maximum, minimum) values at $t = 1.0$ and $t = 1.5$ for $P'_{xy}$, $P'_{xx}$, $P'_{yy}$ are (9.7981E − 05, −9.6920E − 05) for $P'_{xy}$, (9.9110E − 05, −3.1951E − 04) for $P'_{xx}$, (−4.8594E − 01, −4.8627E − 01) for $P'_{yy}$, and (9.8051E − 05, −1.0004E − 04) for $P'_{xy}$, (9.9198E − 05, −3.1943E − 04) for $P'_{xx}$, (−4.8593E − 01, −4.8627E − 01) for $P'_{yy}$, respectively.**

acoustic-vortex interaction. Finally, it should be pointed out that the $P'_{ij}$ behavior is similar for other lower $M_\infty$ cases calculated. Therefore, $P'_{ij}$ could indeed be taken as an indicator of the extent of the nonlinear behavior of the problem.

## VI. Conclusions

The objective of the present study is to extend the BGK-type modeled Boltzmann equation to simulate aeroacoustic problems to directly resolve the nonlinear interactions between aerodynamics and aeroacoustics. To accomplish this objective, improvement of the BGK model is made to relax the $M \ll 1$ assumption inherent in the adoption of the Maxwellian distribution for the equilibrium particle distribution function $f^{eq}$ and its lattice counterpart. The present proposal derives an $f^{eq}$ by imposing constraints related to the exact recovery of the Euler equations without having to invoke the $M \ll 1$ assumption. The function thus derived consists of a leading term given by a modified Maxwellian, and three other terms that are moments of the particle velocity over the whole velocity space. This function reduces exactly to the Maxwellian distribution for the case of a monatomic gas with only the translational energy mode considered. A corresponding lattice $f^{eq}$ is also derived without assuming the inner product of the particle velocity and the macrofluid velocity to be small. Consequently, the derived lattice $f^{eq}$ is not subject to $M \ll 1$ either. Further, the BGK model is extended to diatomic gas, and the approach used to accomplish that is to consider the rotational degree of freedom in the internal energy. This extension allows the ideal gas law to be correctly recovered.

This lattice $f^{eq}$ is applied to simulate two benchmark aeroacoustic problems: one is the propagation of a circular pressure pulse in a quiescent fluid, and another is the propagation of a pressure, a vorticity, and an entropy pulse in a uniform stream with $M_\infty = 0.9$. The LBM using a D2Q9 lattice model is applied to simulate these two problems. Together, these two cases test the ability of the lattice $f^{eq}$ and a D2Q9 model to replicate the isotropic behavior and the complicated interaction of aerodynamics and aeroacoustics at $M_\infty = 0.9$. The calculated results compared very favorably with DNS simulations obtained by solving the Euler equations directly using a sixth-order-accurate finite difference scheme. The error norms between the improved LBM and DNS solutions are equal to or smaller than those previously determined using a D2Q13 lattice model. The calculated $P'_{ij}$ is essentially zero for the circular pulse case, whereas their magnitudes are on the same order as the $u$ fluctuations for the three pulses in a uniform stream case. This suggests that the modified $f^{eq}$ and its lattice counterpart could model the basic particle–particle interaction physics sufficiently well to reflect the overall nonlinear behavior of the three pulses in a uniform stream case. Therefore, the improved LBM is a viable alternative to the DNS scheme for simulating aeroacoustic problems.

## Acknowledgments

Support from the Research Grants Council of the Government of the Hong Kong Special Administrative Region Government given under grant numbers PolyU1/02C, PolyU5303/03E, and PolyU5272/04E, and from the Hong Kong Polytechnic University under grant numbers A-PA2U and A-PA5U is gratefully acknowledged.

## References

[1] Tam, C. K. W., "Computational Aeroacoustics: Issues and Methods," *AIAA Journal*, Vol. 33, No. 10, 1995, pp. 1788–1796.

[2] Lele, S. K., "Compact Finite Schemes with Spectral-Like Resolution," *Journal of Computational Physics*, Vol. 103, No. 1, 1992, pp. 16–42. doi:10.1016/0021-9991(92)90324-R

[3] Tam, C. K. W., and Webb, J. C., "Dispersion-Relation-Preserving Finite Difference Schemes for Computational Aeroacoustics," *Journal of Computational Physics*, Vol. 107, No. 2, 1993, pp. 262–281. doi:10.1006/jcph.1993.1142

[4] Visbal, M. R., and Gaitonde, D. V., "High-Order-Accurate Methods for Complex Unsteady Subsonic Flows," *AIAA Journal*, Vol. 37, No. 10, 1999, pp. 1231–1239.

[5] Colonius, T., and Lele, S. K., "Computational Aeroacoustics: Progress on Nonlinear Problems of Sound Generation," *Progress in Aerospace Sciences*, Vol. 40, No. 6, 2004, pp. 345–416. doi:10.1016/j.paerosci.2004.09.001

[6] Chen, H., Chen, S., and Matthaeus, W. H., "Recovery of the Navier–Stokes Equations Using a Lattice-Gas Boltzmann Method," *Physical Review A*, Vol. 45, No. 8, 1992, pp. R5339–R5342. doi:10.1103/PhysRevA.45.R5339

[7] Chen, S., and Doolen, G. D., "Lattice Boltzmann Method for Fluid Flows," *Annual Review of Fluid Mechanics*, Vol. 30, Jan. 1998, pp. 329–364. doi:10.1146/annurev.fluid.30.1.329

[8] Succi, S., *Lattice Boltzmann Equation for Fluid Dynamics and Beyond*, Oxford Univ. Press, Oxford, England, U.K., 2001.

[9] Bhatnagar, P. L., Gross, E. P., and Krook, M., "Model for Collision Processes in Gases, 1: Small Amplitude Processes in Charged and Neutral One-Component Systems," *Physical Review*, Vol. 94, No. 3, 1954, pp. 511–525. doi:10.1103/PhysRev.94.511

[10] Buick, J. M., Greated, C. A., and Campbell, D. M., "Lattice BGK Simulation of Sound Waves," *Europhysics Letters*, Vol. 43, No. 3, 1998, pp. 235–240. doi:10.1209/epl/i1998-00346-7

[11] Kataoka, T., and Tsutahara, M., "Lattice Boltzmann Model for the Compressible Navier–Stokes Equations with Flexible Specific-Heat Ratio," *Physical Review E (Statistical Physics, Plasmas, Fluids, and Related Interdisciplinary Topics)*, Vol. 69, No. 3, 1999, Article No. 035701.

[12] Buick, J. M., Buckley, C. L., Greated, C. A., and Gilbert, J., "Lattice Boltzmann BGK Simulation of Nonlinear Sound Waves: The Development of a Shock Front," *Journal of Physics A: Mathematical and General*, Vol. 33, No. 21, 2000, pp. 3917–3928. doi:10.1088/0305-4470/33/21/305

[13] Tsutahara, M., Kataoka, T., Takada, N., Kang, H. K., and Kurita, M., "Simulations of Compressible Flows by Using the Lattice Boltzmann and the Finite Difference Lattice Boltzmann Methods," *Computational Fluid Dynamics Journal*, Vol. 11, No. 1, 2002, pp. 486–493.

[14] Li, X. M., Leung, R. C. K., and So, R. M. C., "One-Step Aeroacoustics Simulation Using Lattice Boltzmann Method," *AIAA Journal*, Vol. 44, No. 1, 2006, pp. 78–89. doi:10.2514/1.15993

[15] Li, X. M., So, R. M. C., and Leung, R. C. K., "Propagation Speed, Internal Energy and Direct Aeroacoustics Simulation Using Lattice Boltzmann Method," *AIAA Journal*, Vol. 44, No. 12, 2006, pp. 2896–2903. doi:10.2514/1.18933

[16] Kam, E. W. S., So, R. M. C., and Leung, R. C. K., "Lattice Boltzmann Method Simulation of Aeroacoustics and Nonreflecting Boundary Conditions," *AIAA Journal*, Vol. 45, No. 7, 2007, pp. 1703–1712. doi:10.2514/1.27632

[17] Chapman, S., and Cowling, T. G., *Mathematical Theory of Non-Uniform Gases*, 3rd ed., Cambridge Univ. Press, Cambridge, England, U.K., 1990.

[18] Lele, S. K., "Direct Numerical Simulations of Compressible Turbulent Flows: Fundamentals and Applications," *Transition, Turbulence and Combustion Modeling*, edited by A. Hanifi, P. H. Alfredsson, A. V. Johansson, and D. S. Hennigson, Kluwer Academic, London, 1998, Chap 7, pp. 424–429.

[19] Wang Chang, C. S., Uhlenbeck, G. E., and deBoer, J., *Studies in Statistical Mechanics*, edited by J. deBoer, and G. E. Uhlenbeck, Vol. 2, Wiley, New York, 1964.

[20] Harris, S., *Introduction to the Theory of the Boltzmann Equation*, Dover, New York, 1999, Chaps. 1–4.

[21] Morse, T. F., "Kinetic Model for Gases with Internal Degrees of Freedom," *Physics of Fluids*, Vol. 7, No. 2, 1964, pp. 159–169. doi:10.1063/1.1711128

[22] Holway, L. H., "New Statistical Models for Kinetic Theory: Methods of Construction," *Physics of Fluids*, Vol. 9, No. 9, 1966, pp. 1658–1673. doi:10.1063/1.1761920

[23] Prendergast, K. H., and Xu, K., "Numerical Hydrodynamics from Gas-Kinetic Theory," *Journal of Computational Physics*, Vol. 109, No. 1, 1993, pp. 53–66. doi:10.1006/jcph.1993.1198

[24] Xu, K., and Prendergast, K. H., "Numerical Navier–Stokes Solution from Gas-Kinetic Theory," *Journal of Computational Physics*, Vol. 114, No. 1, 1994, pp. 9–17. doi:10.1006/jcph.1994.1145

[25] Xu, K., "Gas-Kinetic BGK Scheme for the Navier–Stokes Equations and its Connection with Artificial Dissipation and Godunov Method," *Journal of Computational Physics*, Vol. 171, No. 1, 2001, pp. 289–335. doi:10.1006/jcph.2001.6790

[26] Sterling, J. D., and Chen, S., "Stability Analysis of Lattice Boltzmann Methods," *Journal of Computational Physics*, Vol. 123, No. 1, 1996, pp. 196–206. doi:10.1006/jcph.1996.0016

[27] Holberg, O., "Computational Aspects of the Choice of Operator and Sampling Interval for Numerical Differentiation in Large-Scale Simulation of Wave Phenomena," *Geophysical Prospecting*, Vol. 35, No. 6, 1987, pp. 629–655. doi:10.1111/j.1365-2478.1987.tb00841.x

[28] Yan, G., Chen, Y., and Hu, S., "Simple Lattice Boltzmann Model for Simulating Flows with Shock Wave," *Physical Review E (Statistical Physics, Plasmas, Fluids, and Related Interdisciplinary Topics)*, Vol. 59, No. 1, 1999, pp. 454–459. doi:10.1103/PhysRevE.59.454

[29] Shi, W., Shyy, W., and Mei, R., "Finite-Difference-Based Lattice Boltzmann Method for Inviscid Compressible Flows," *Numerical Heat Transfer, Part B: Fundamentals*, Vol. 40, No. 1, 2001, pp. 1–21. doi:10.1080/104077901300233578

[30] Sun, C., "Lattice-Boltzmann Models for High-Speed Flow," *Physical Review E (Statistical Physics, Plasmas, Fluids, and Related Interdisciplinary Topics)*, Vol. 58, No. 6, 1998, pp. 7283–7287. doi:10.1103/PhysRevE.58.7283

[31] Li, X. M., "Computational Aeroacoustics Using Lattice Boltzmann Model," Ph.D. Thesis, Mechanical Engineering Dept., Hong Kong Polytechnic Univ., Hong Kong, 2006.

[32] Shan, X., and He, X., "Discretization of the Velocity Space in the Solution of the Boltzmann Equation," *Physical Review Letters*, Vol. 80, No. 1, 1998, pp. 65–68. doi:10.1103/PhysRevLett.80.65

[33] Philippi, P. C., Hegele, L. A., Jr., dos Santos, L. O. E., and Surmas, R., "From the Continuous to the Lattice Boltzmann Equation: The Discretization Problem and Thermal Models," *Physical Review E (Statistical Physics, Plasmas, Fluids, and Related Interdisciplinary Topics)*, Vol. 73, May 2006, pp. 056702. doi:10.1103/PhysRevE.73.056702

[34] Wolf-Gladrow, D. A., *Lattice-Gas Cellular Automata and Lattice Boltzmann Models: An Introduction*, Springer–Verlag, Berlin, 2000, Chap. 5.

[35] Cao, N. S., Chen, S., Jin, S., and Martinez, D., "Physical Symmetry and Lattice Symmetry in the Lattice Boltzmann Method," *Physical Review E (Statistical Physics, Plasmas, Fluids, and Related Interdisciplinary Topics)*, Vol. 55, No. 1, 1997, pp. R21–R24. doi:10.1103/PhysRevE.55.R21

[36] Mei, R., and Shyy, W., "On the Finite Difference-Based Lattice Boltzmann Method in Curvilinear Coordinates," *Journal of Computational Physics*, Vol. 143, No. 2, 1998, pp. 426–448. doi:10.1006/jcph.1998.5984

[37] d'Humieres, D., "Generalized Lattice-Boltzmann Equations," *Rarefied Gas Dynamics: Experimental Techniques and Physical Systems*, edited by B. D. Shizgal, and D. P. Weaver, Vol. 159, Progress in Astronautics and Aeronautics, AIAA, Washington, D.C., 1992, pp. 450–458.

[38] d'Humieres, D., Bouzidi, M., and Lallemand, P., "Thirteen-Velocity Three-Dimensional Lattice Boltzmann Model," *Physical Review E (Statistical Physics, Plasmas, Fluids, and Related Interdisciplinary Topics)*, Vol. 63, No. 6, 2001, p. 066702. doi:10.1103/PhysRevE.63.066702

[39] Visbal, M. R., and Gaitonde, D. V., "Very High-Order Spatially Implicit Schemes for Computational Acoustics on Curvilinear Meshes," *Journal of Computational Acoustics*, Vol. 9, No. 4, 2001, pp. 1259–1286.

X. Zhong
*Associate Editor*